PHYSICAL REVIEW B **83**, 184501 (2011)

Temperature distribution in a large $Bi_2Sr_2CaCu_2O_{8+\delta}$ mesa

A. Yurgens
Department of Microtechnology and Nanoscience (MC2), Chalmers University of Technology, SE-412 96 Göteborg, Sweden
(Received 8 April 2010; revised manuscript received 28 February 2011; published 5 May 2011)

Joule heating in large $Bi_2Sr_2CaCu_2O_{8+\delta}$ mesas was numerically analyzed while taking into account typical thermal conductivities and their temperature dependences of all the materials involved in heat dissipation and removal. Such mesas are used in experiments on THz-range radiation. The analysis shows that the temperature increases with bias current and is distributed unevenly along the mesas. The temperature of the mesa's middle part can even exceed T_c at sufficiently high bias. The overall current-voltage characteristics are also calculated self-consistently, showing a negative differential conductance in a wide range of currents.

DOI: 10.1103/PhysRevB.83.184501 PACS number(s): 74.25.Sv, 74.50.+r, 74.72.−h

The ac Josephson effect provides the basis for superconducting high-frequency detectors and tunable radiation sources with a voltage-to-frequency conversion parameter involving only fundamental constants. Josephson junctions made of high-temperature superconductors (HTSs) allow for such devices operating in a wide temperature range ∼4–90 K and high frequencies including the THz band.[1,2] Synchronization (or phase locking) of many Josephson junctions is needed to boost the radiation power.[3,4] The high-frequency radiation from arrays of the so-called intrinsic Josephson junctions (IJJs)[5] in $Bi_2Sr_2CaCu_2O_{8+\delta}$ (Bi2212) was seen in several works.[6,7] However, the radiation was not strong, indicating the absence of junction phase locking.

A THz-range emission has been detected recently from large Bi2212 mesas containing several hundred IJJs.[8,9] The radiation is relatively intense, indicating a high level of junction synchronization. Because the radiation frequency has been found to be inversely proportional to the mesa width, it is natural to include cavity resonances for the explanation of the synchronization.[10–14] The large mesa area means that the bias current needed to keep IJJs in the voltage state is high. The overall Joule heating is essential at this bias, which requires analysis of the heat balance and cooling efficiency in the mesas. A simplified analysis of the heating using Newton's law of cooling does not give the spatial variation of the mesa temperature. It also results in a significant underestimation of the maximum temperature rise in such mesas.[15] In a standalone Bi2212 single crystal with small width and height corresponding to many IJJs ($\sim 10^4$), different junctions are predicted to be synchronized by the electromagnetic field generated by the junction oscillations themselves.[16] For a certain geometry, such a source is found to be less prone to Joule heating[17] but, to the best of my knowledge, has so far not been realized in practice.

In this work, I calculate the temperature distribution $T(\mathbf{r})$ in large mesas by numerically solving the nonlinear diffusion equation[18]

$$\nabla\big(-k[T(\mathbf{r})]\nabla T(\mathbf{r})\big) = \rho[T(\mathbf{r})]j(\mathbf{r})^2 \qquad (1)$$

for mesas of typical geometry and realistic thermal conductivities $k(T)$ of all the materials involved in the heat generation and removal, as well as their temperature dependences and anisotropy. Here, $\mathbf{r}$, j, and ρ are the coordinate, current density, and anisotropic resistivity, respectively.

Figure 1 schematically shows a model device comprising a mesa on top of a Bi2212 single crystal. The crystal is taken to be 1×1 mm^2 in area and either 20 or 40 μm thick. The single crystal is attached to a sapphire substrate with a 20-μm-thick polymethylmethacrylate (PMMA) glue layer. Due to the high thermal conductivity of sapphire, the substrate surface is assumed to be always at the bath temperature T_0. There is no cooling gas around the sample, meaning that the heat dissipated in the mesa can only escape through the underlying single crystal and the PMMA layer. The calculations are made for one and the same length of the mesa, $l = 300$ μm. The mesa width w (the height h) is either 50 or 100 μm (1 or 2 μm). A 100-nm gold thin film is deposited on top of the mesa and the front part of the single crystal, making up the bias electrodes (see Fig. 1). There is no interim resistive layer between the electrodes and Bi2212. All the simulations have been made using the finite-element software package COMSOL.[18]

The anisotropic thermal conductivity $k(T)$ of Bi2212 single crystals was measured in a number of works, predominantly along the ab plane.[19–22] To the best of my knowledge, there exist only two measurements of the thermal conductivity in the c-axis direction.[23,24] It was found that the ratio $k_{ab}/k_c \sim 6$ in a wide temperature range and increases to 8 at low temperatures.[23] In the calculations, I use k_{ab} for pure Bi2212 adopted from Ref. 22 and take $k_c = k_{ab}/10$. It is also assumed that there is no reflection of phonons at the material interfaces.[25]

The ab-plane resistivity of Bi2212 is taken to be linear in temperature, $\rho_{ab} = \theta(T - T_c,\delta T)T/75$ ($\mu\Omega$ m), where $\theta(x,\delta x)$ is the Heaviside step function smeared over the interval δx and $T_c = 86$ K is the superconducting critical temperature of the optimally doped Bi2212. The Heaviside function is used to mimic the transition to the normal-metal state when the local temperature exceeds T_c. The current-induced transitions within individual CuO planes[26] are ignored in these calculations.

There is no universal c-axis resistivity $\rho_c(T)$ for Bi2212 because of its strong dependence on the oxygen content and disorder.[27] Below T_c, ρ_c can be obtained from the subgap resistance R_{sg} of IJJs in the limit $I,V \to 0$.[28,29] In the present calculations, $\rho_c(T)$ has been adopted from Ref. 8 and extrapolated to low temperatures while keeping it smaller than ~ 10 Ω m to mimic a tendency to saturation observed in several experiments.[28–30]

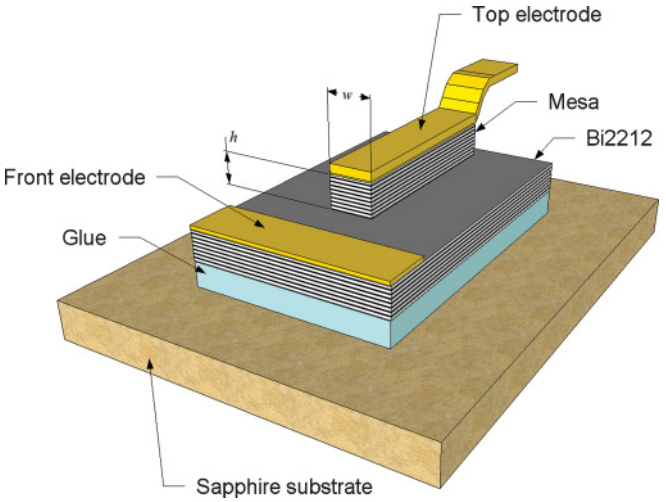

FIG. 1. (Color online) Schematic view of a mesa used in the calculations. The mesa height $h = 1$ or 2 μm; the width $w = 50$ or 100 μm; the mesa length is 300 μm; the Bi2212 single-crystal thickness is 20 or 40 μm, and the glue thickness is 20 μm. Not to scale.

The thermal conductivity of gold is calculated from an experimentally measured resistivity of a 100-nm thick gold thin film by using the Wiedemann-Franz law. The thermal conductivity of the PMMA layer is adopted from Ref. 31. Thermal conductivity of other possible epoxies and glues is not very different from that of PMMA.[32]

Two-dimensional temperature distributions calculated for several current densities in a mesa 50 μm wide are shown in Fig. 2(a). The distributions correspond to the horizontal plane at half the mesa height. The temperature is spatially nonuniform and increases with current. For high current densities, the temperature can even exceed T_c in the middle part of the mesa. The thick contour lines indicate the boundary between the superconducting and normal-metal regions. The normal-metal part grows with current and the superconducting mesa eventually breaks up into two smaller ones connected by the common electrode and the normal-state region.

Figures 2(b) and 2(c) show a side-by-side comparison of the temperature-distribution patterns obtained in the present calculations and recent laser-microscopy experiments.[33,34] The latter shows the top-electrode voltage variations due to additional heating from a small laser spot which is scanned over the mesa structure. The spot is $\sim$2 μm in diameter and is estimated to raise the local temperature in the spot by a few kelvins.[33]

The laser-microscopy patterns reveal distinct rings with their diameter increasing with bias current. The rings resemble thick contour lines of the simulations that correspond to $T = T_c$. It is fully reasonable to expect large resistance variations at local places where the temperature is close to T_c, giving rise to larger signals than from other parts of the mesa.

At some high bias current the laser microscope reveals the presence of some kind of standing waves, giving a very strong response in the experiment [see the pink spots in Fig. 2(c)]. The origin of the spots is not totally clear and is now being debated.[33,34] This is, however, beyond the scope of the present work and will not be discussed here.

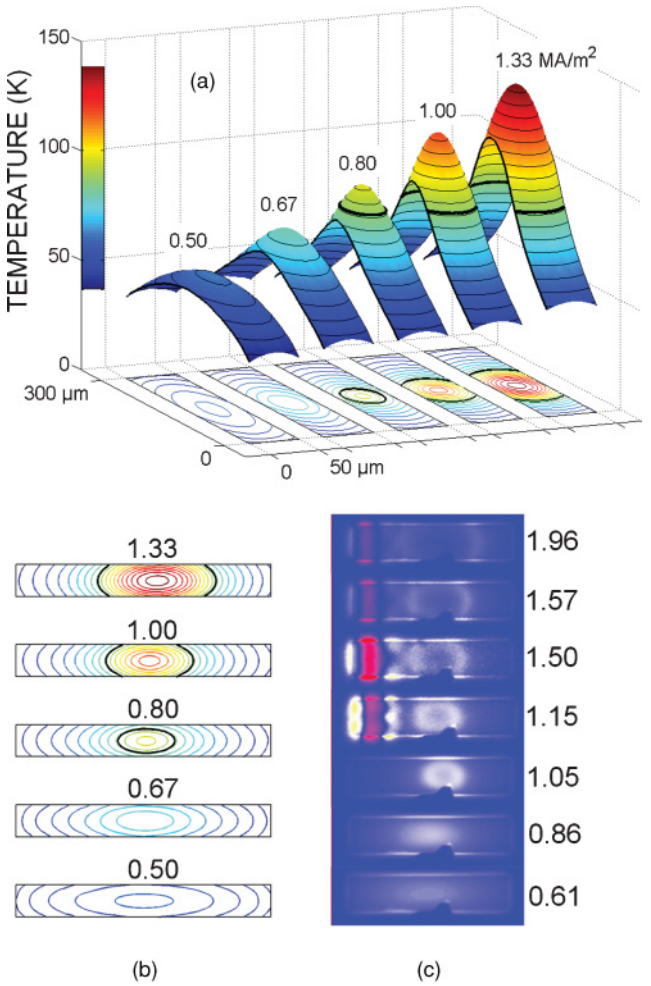

FIG. 2. (Color online) (a) The temperature distribution in the mesa 50 μm wide at different current densities. The contour lines are drawn for every 5 K. $T = T_c$ is marked by the thick lines. (b) and (c) A side-by-side comparison of the calculated pattern of the temperature distribution as in (a) with the experimental laser-microscopy image of the 70×330 μm^2 large mesa. The false-color scale indicates the mesa-voltage variations due to the local additional heating in the laser spot which is scanned over the mesa surface. The current densities in MA/m^2 are indicated. The image in (c) is reproduced with permission from the supplementary information of H.B. Wang *et al.*, Phys. Rev. Lett. **102**, 017006 (2009) (Ref. 33); © 2009 American Physical Society.

Figure 3(a) shows the current-voltage characteristics (I-V's) for a mesa 50 μm wide at different bath temperatures from 10 to 80 K with 10-K intervals. The I-V's have been calculated self-consistently, assuming the three-dimensional heat- and electrical-current distributions. The dashed line indicates the boundary at which the maximum temperature $T_{\max}$ of the temperature distribution reaches T_c. The curves reproduce experimental I-V's qualitatively well.[8] It is also seen that the backbending decreases with T_0, also in accordance with experiments. Figure 3(b) shows the calculated I-V's for different mesas at $T_0 = 10$ K. The triple numbers along each line indicate the mesa width, height, and thickness of the underlying single crystal. The solid dots indicate the I-V points where $T_{\max} = T_c$. It is the mesa sizes that largely govern the

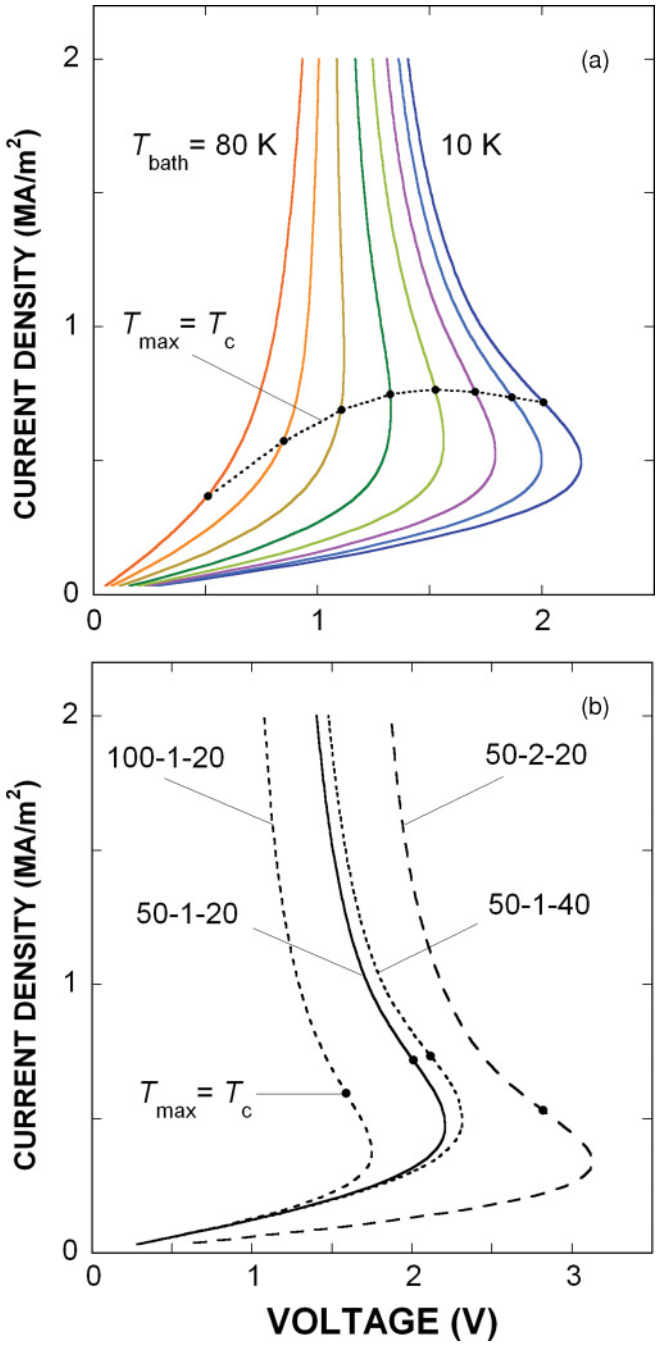

FIG. 3. (Color online) (a) The *I-V*'s of the 50-μm-wide mesa at T_0 from 10 to 80 K with 10-K intervals (solid lines). The dashed line indicates a boundary at which T_{max} reaches T_c. (b) The *I-V*'s at $T_0 = 10$ K. The triple numbers indicate the mesa width, the mesa height, and the thickness of the underlying single crystal (in μm). The dots mark the *I-V* points where $T_{max} = T_c$.

maximum temperature whereas the thickness of the underlying single crystal is of minor importance. Indeed, compare curve "50-1-20" versus "50-1-40," and "50-1-20" versus "50-2-20" or "100-1-20." From Fig. 3(b) it is seen that $T_{max} = T_c$ at the bias current slightly above the current I_g corresponding to the local voltage maximum [at which $dV/dI(I_g) = 0$]. This is in agreement with the direct measurements of the mesa temperature.[35]

A simple self-consistent analysis of *I-V*'s in the presence of Joule heating can be made using Newton's law of cooling:

$$T = T_0 + \alpha I V(I,T), \tag{2}$$

$$V(I,T) = I R(T), \tag{3}$$

where α and R are the thermal and electrical resistances, respectively. $R(T)$ here is assumed to be independent of I, i.e., *I-V*'s are linear (ohmic) in the absence of self-heating while $\alpha =$ const with respect to both current and temperature. All the nonlinearities of the overall *I-V*'s are assumed to be due to the self-heating alone.

When the temperature changes, so do the thermal conductivities of all the materials involved in the heat transfer from the junctions. This means that α changes, too, and the simplicity of Eq. (2) gets broken. It should then be replaced by a more realistic Eq. (1). However, the *I-V*'s can, quite confidently, be still regarded as linear in the absence of self-heating [Eq. (3)]. Indeed, for large and high mesas, the self-heating becomes essential already at currents much smaller than the superconducting critical current. A mesa 1 μm high has $\sim$700 IJJs in a series. The sum-gap voltage would reach the maximum value $V_{gm} \sim 40$ V assuming a typical gap voltage $2\Delta/e = 60$ mV per junction and no heating. The corresponding current $I_{gm} = V_{gm}/R = 100$ mA, assuming the ohmic subgap resistance $R \sim 400\ \Omega$ estimated from the c-axis resistivity $\rho_c \sim 600\ \Omega$ cm. The experimental voltage range is $\sim$20 times smaller than V_{gm} due to self-heating and semiconductorlike $R(T)$. The range of currents used in the THz-emission measurements is at least two times smaller than I_{gm} and would correspond to voltages $\leqslant V_{gm}/2$ in the absence of heating. *I-V*'s can be regarded as linear in this range. Experiments on submicrometer shallow mesas which are least affected by self-heating show that this is an acceptable assumption.[36] It should be noted though that Eq. (3) is only important for calculation of the self-consistent *I-V*'s. The nonuniform temperature distribution can be obtained even in the case of uniform power dissipation and without any assumptions regarding the mesa resistance.

The temperature distribution across the vertical middle section of the mesa and the underlying single crystal at $j = 1.33$ MA/cm^2 is shown in Fig. 4. The dashed-dotted line marks the isotherm $T = T_c$. The normal-state region extends by $\sim$10 μm deep into the pedestal of the mesa at high current. This means that cooling of the mesa becomes the most effective for a pedestal that is thinner than that size.

The fact that the mesa temperature can exceed T_c at $I > I_g$ where the intense THz radiation has been observed makes it reasonable to suggest that the heating plays an active role in the synchronization of IJJs in large mesas. Indeed, the normal-state part of the mesa at $I > I_g$ can effectively create a shunting resistor for the rest of the mesa which is still in the superconducting state. It is well known that a load impedance common to all the Josephson junctions in a series array can stimulate their synchronization.[37] The difference with previous works (e.g., Ref. 37) is that IJJs are shunted by a *distributed* resistance in the overheated mesa (see Fig. 4). Every IJJ is connected not only to its two neighbors but to the shunt as well. Then, the current is not necessarily one and the same for all the junctions. Nonetheless, preliminary lumped-element

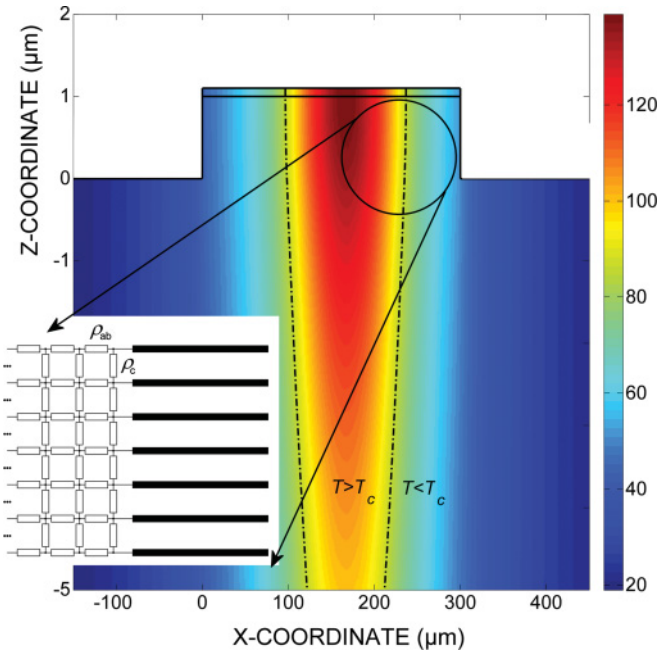

FIG. 4. (Color online) The temperature distribution across the vertical middle section of the mesa and the underlying single crystal at $j = 1.33\ \mathrm{MA/m^2}$. The dashed-dotted lines mark the isotherm $T = T_c$ while the solid horizontal line marks the boundary between the mesa and the electrode. The inset schematically shows a simplified picture of the resistively shunted section of the mesa. The equivalent shunting circuitry is an infinite matrix of resistors representing the in- and out-of-plane resistivities.

simulations have shown that the synchronization is possible even in this case (see the Appendix).

In summary, self-heating in large-area and high mesas that are used in experiments on powerful THz emission from IJJs is analyzed by numerically solving the diffusion equation. The current-voltage characteristics are calculated self-consistently, showing regions of negative differential conductance. Particular mesa geometry and the temperature dependences of all the electrical and thermal material parameters are included in the calculations. The calculations reveal that the mesa temperature is not only significantly higher than the bath temperature, but it is strongly nonuniform along the mesa length and width. The middle part of the mesa can be overheated even above T_c at a high bias that is consistent with the laser-microscopy experiments. The normal-state regions make up an effective resistive shunting for the rest of the mesa that can play an important role in the synchronization of IJJs.

ACKNOWLEDGMENTS

I acknowledge support from the Swedish Research Council through the Linnaeus centrum "Engineering quantum systems" and wish to thank J. F. Schneiderman for reading the manuscript.

APPENDIX: SYNCHRONIZATION BY A DISTRIBUTED LOAD

Here, I show that it is, in principle, possible to achieve synchronization of Josephson junctions by a *distributed* load. The normal-state (overheated) regions of a large Bi2212 mesa containing IJJs can therefore be relevant for the recently observed THz emission from such mesas.

Synchronization of many Josephson junctions connected in series and having a common load was thoroughly studied previously.[38] In that case, the load is connected to the first and the last junctions of the array and the bias current is split in two parts, one flowing in the load and another in the junction array. In this geometry, the Josephson junctions share the same current. To the best of my knowledge, a situation when every junction is connected to the distributed load has not been considered previously.[39] The current is now not necessarily one and the same for all the junctions in the array, and it is not rational to expect the synchronization in general. However, the particular case of large Bi2212 mesas is somewhat special. The bias current is spread over the extended superconducting regions of the mesa and also the parts driven to the normal state by Joule heating. The current density does not change much along the mesa area and is largely constant across its thickness at a given ab-plane spot. The current-density pattern through the extended Josephson junctions is thus quite uniform, which makes the synchronization more feasible.

I model the system by a lumped-element approximation shown in Fig. 5. The number of Josephson junctions is $N = 15$ and the number of elements in the distributed load in the "horizontal" direction is $M = 10$. The choice of N and M is not crucial; the synchronization has also been checked for $M = 2$, giving the similar results. The "vertical" (R_v) and "horizontal" (R_h) resistors represent the c-axis and ab-plane resistivities, respectively. The capacitors represent intrinsic capacitance (C_m) between the planar electrodes of IJJs. There are also bias resistors (R_b) both at the top and bottom of the load matrix. Both the vertical and horizontal resistors are set to depend on the position in the horizontal direction, in qualitative agreement with the strong lateral temperature gradient in the mesa [see Fig. 2(a)] and the temperature-dependent c-axis and

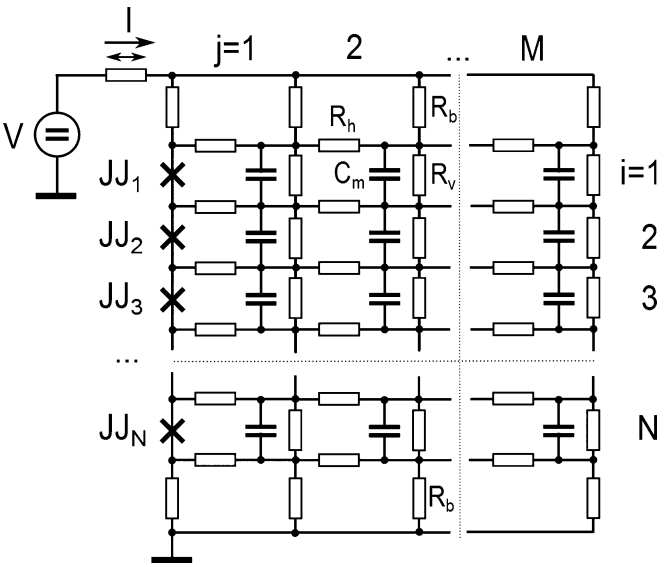

FIG. 5. The lumped-element circuitry to simulate behavior of Josephson junctions in an array connected to a load composed of distributed resistance and capacitance.

ab-plane resistivities. $R_{hj} = 10j$, $R_{bj} = 0.11$–$0.005j$, $R_{vj} = 8200$–$400j$; ($j = 1 \ldots M$) (all in units of the shunt resistance R of the individual Josephson junction); $C_m = 0.1 = \text{const}$ (in units of the shunt capacitance C of the individual Josephson junction). These values have more or less arbitrarily been guessed in attempt to mimic the real situation with no intention to exactly match the properties of IJJs. For the present simulations which only aim at a qualitative yes or no answer, the particular values are not important. It has been checked that the synchronization can also be achieved when the resistances are the same for each of the directions.

A Josephson junction is described by the shunted-junction model,

$$\frac{\hbar C}{2eI_c}\ddot{\phi} + \frac{\hbar C}{2eI_c RC}\dot{\phi} + \sin(\phi) = \frac{I}{I_c}, \tag{A1}$$

which can be rewritten with help of the following definitions,

$$V = \frac{\hbar}{2e}\dot{\phi}, \quad \omega_p = \sqrt{\frac{2eI_c}{\hbar C}}, \quad Q = \omega_p RC, \tag{A2}$$

to read

$$\frac{Q}{\omega_p}\frac{\dot{V}}{R\,I_c} + \frac{V}{R\,I_c} + \sin\left(Q\int\frac{V}{R\,I_c}dt\right) = \frac{I}{I_c}, \tag{A3}$$

where ϕ is the phase; R, C, and Q are the junction shunt resistance, shunt capacitance, and quality factor, respectively; ω_p is the Josephson plasma frequency; I is the current and I_c is the superconducting critical current.

Assuming that time is measured in units of the inverse plasma frequency ω_p, voltage in units of RI_c, and current in units of I_c, we arrive at the following equation:

$$Qv' + v + \sin\left(Q\int v\,d\tau\right) = \tilde{I}, \tag{A4}$$

which is then modeled by Simulink® (www.mathworks.com) elementary parts (see Fig. 6). The initial phases of individual Josephson junctions are set to be normally distributed around zero with a standard deviation of 1 rad by correspondingly adjusting the initial conditions of the integrators. The time evolution of the junction phases for $V = 20$ is shown in Fig. 7. The average phase $\bar{\phi}(\tau) = \sum\phi_i(\tau)/N$ (a linearly increasing function) has been subtracted to resolve details of individual $\phi_i(\tau)$ dependences.

It is seen that the initial chaotic behavior settles down after some time and the $\phi_i(\tau > 50)$ dependences show steady

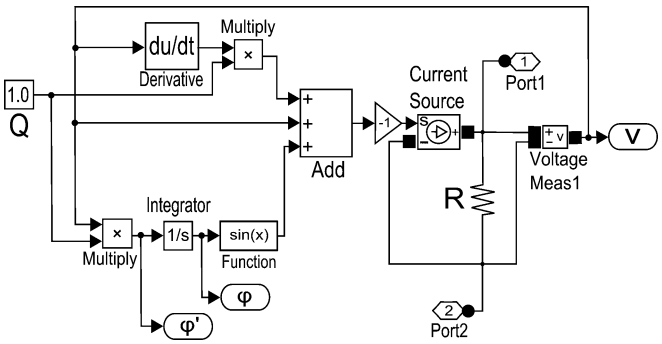

FIG. 6. The Simulink model of a Josephson junction used in the simulations.

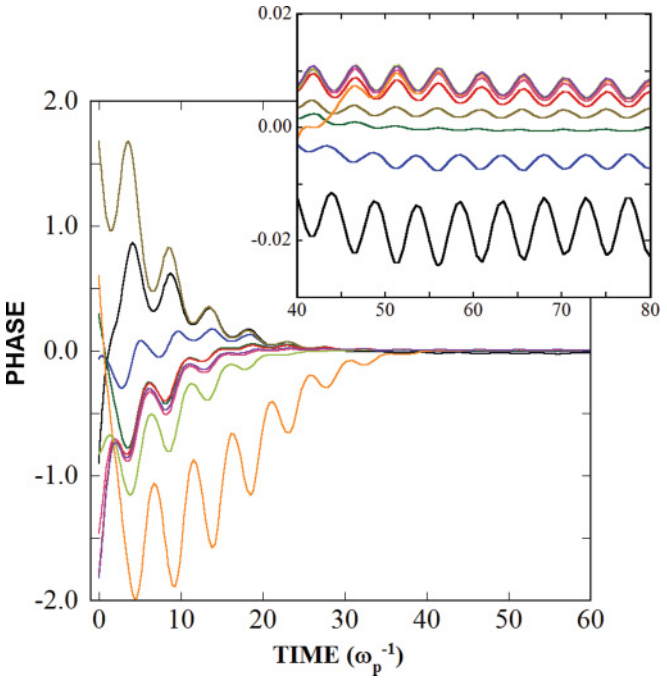

FIG. 7. (Color online) The evolution of individual phases with time at $V = 20$. The average phase has been subtracted. The inset shows a zoomed-in part of the synchronized state.

patterns. All the Josephson junctions are largely in phase. There is, however, a small-amplitude phase swinging around the linearly increasing $\bar{\phi}(\tau)$; this only slightly dephases the junctions. The fast Fourier transform (FFT) spectra of the time-dependent net current I for $\tau > 200$ (to exclude initial chaotic stage) is shown in the inset of Fig. 8. The spectra show narrow peaks, demonstrating a perfectly sinusoidal character of the ac component of the net current.

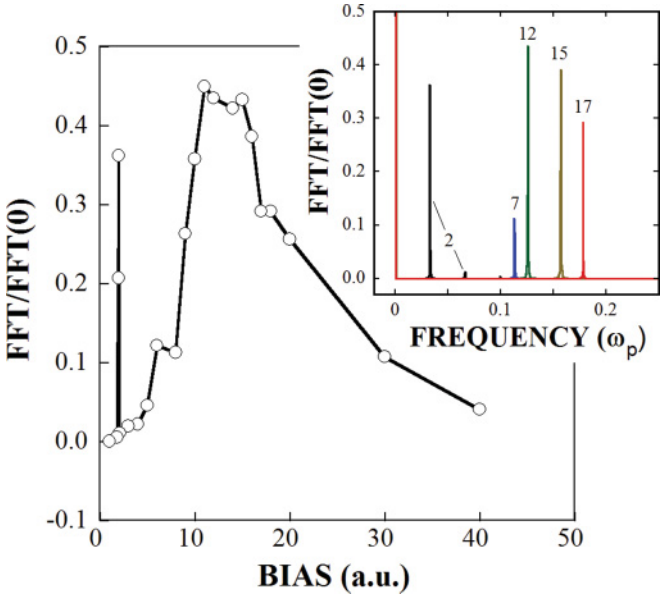

FIG. 8. (Color online) The ratio of the dominant peak height of the FFT spectrum to its dc component as a function of the dc bias voltage. The inset shows FFT power spectra of the net current I for various bias voltages indicated.

The ratio of the dominant ac component of the FFT spectrum to the dc one can be used to characterize the effectiveness of the synchronization. Figure 8 shows how this ratio changes with bias. The maximum height (efficiency) is reached in the range $V = 12$–16, with rather a sharp onset at $V \sim 10$. It should be noted that the load matrix resistors are taken to be independent of current, unlike the real situation with large mesas where the material resistivities are functions of temperature and, hence, Joule heating (i.e., current). The temperature distribution in the mesa depends on the bias and so does the resistivity of its normal-state part (see above). Introducing this dependence in the simulations is expected to narrow down the voltage range at which the synchronization of junctions is considerable. There is also a very narrow region at $V = 2$ where the efficiency is relatively high as well (see Fig. 8), although the particular reason for that is unclear. In real experiments, a powerful radiation has also been observed in a quite narrow window of currents and voltages.[8,9] Moreover, it has been noted that perhaps not all IJJs in the mesa contribute to radiation[8] that can be explained by a trapezoidal cross section of the mesa.[40]

In summary, I have qualitatively shown that a series array of Josephson junctions can be synchronized by a *distributed* load. The synchronization leads to a significant ac component of the net current and, much likely, to efficient emission of radiation. This validates the suggestion that the normal-state part of a large mesa that appears because of Joule heating can be important for synchronization of IJJs in the mesa.

[1] D. Winkler, Y.-M. Zhang, P.-Å. Nilsson, E. A. Stepantsov, and T. Claeson, Phys. Rev. Lett. **72**, 1260 (1994).
[2] J. Edstam and H. K. Olsson, Appl. Phys. Lett. **64**, 2733 (1994).
[3] J. Edstam, P. Larsson, E. A. Stepantsov, and H. K. Olsson, Physica C **235-240**, 3385 (1994).
[4] K. Lee, I. Iguchi, and K. Y. Constantinian, Physica C **320**, 65 (1999).
[5] R. Kleiner, F. Steinmeyer, G. Kunkel, and P. Müller, Phys. Rev. Lett. **68**, 2394 (1992).
[6] K. Lee, W. Wang, I. Iguchi, M. Tachiki, K. Hirata, and T. Mochiku, Phys. Rev. B **61**, 3616 (2000); K. Lee and I. Iguchi, Physica C **367**, 376 (2002).
[7] I. E. Batov, X. Y. Jin, S. V. Shitov, Y. Koval, P. Muller, and A. V. Ustinov, Appl. Phys. Lett. **88**, 262504 (2006).
[8] L. Ozyuzer *et al.*, Science **318**, 1291 (2007).
[9] K. Kadowaki *et al.*, Physica C **468**, 634 (2008).
[10] A. E. Koshelev and L. N. Bulaevskii, Phys. Rev. B **77**, 014530 (2008).
[11] A. E. Koshelev, Phys. Rev. B **78**, 174509 (2008).
[12] S. Lin and X. Hu, Phys. Rev. Lett. **100**, 247006 (2008); Phys. Rev. B **79**, 104507 (2009).
[13] M. Tachiki, S. Fukuya, and T. Koyama, Phys. Rev. Lett. **102**, 127002 (2009).
[14] M. Tsujimoto, K. Yamaki, K. Deguchi, T. Yamamoto, T. Kashiwagi, H. Minami, M. Tachiki, K. Kadowaki, and R. A. Klemm, Phys. Rev. Lett. **105**, 037005 (2010).
[15] C. Kurter *et al.*, IEEE Trans. Appl. Supercond. **19**, 428 (2009).
[16] L. N. Bulaevskii and A. E. Koshelev, Phys. Rev. Lett. **99**, 057002 (2007).
[17] A. Yurgens and L. N. Bulaevskii, Supercond. Sci. Technol. **24**, 015003 (2011).
[18] See [http://www.comsol.com] for details.
[19] N. V. Zavaritsky, A. V. Samoilov, and A. Yurgens, Physica C **169**, 174 (1990).
[20] C. Uher, in *Physical Properties of High Temperature Superconductors III*, edited by D. M. Ginzberg (World Scientific, Singapore, 1992), p. 159.
[21] K. Krishana, N. P. Ong, Q. Li, G. D. Gu, and N. Koshizuka, Science **277**, 83 (1997).
[22] Yoichi Ando, J. Takeya, Y. Abe, K. Nakamura, and A. Kapitulnik, Phys. Rev. B **62**, 626 (2000).
[23] M. F. Crommie and A. Zettl, Phys. Rev. B **43**, 408 (1991).
[24] X. D. Wu, G. S. Kino, J. T. Fanton, and A. Kapitulnik, Rev. Sci. Instrum. **64**, 3321 (1993).
[25] R. E. Peterson and A. C. Anderson, J. Low Temp. Phys. **11**, 639 (1973).
[26] L. X. You, A. Yurgens, and D. Winkler, Phys. Rev. B **71**, 224501 (2005).
[27] T. Watanabe, T. Fujii, and A. Matsuda, Phys. Rev. Lett. **79**, 2113 (1997).
[28] Yu. I. Latyshev, T. Yamashita, L. N. Bulaevskii, M. J. Graf, A. V. Balatsky, and M. P. Maley, Phys. Rev. Lett. **82**, 5345 (1999).
[29] A. Yurgens, D. Winkler, N. V. Zavaritsky, and T. Claeson, Phys. Rev. Lett. **79**, 5122 (1997).
[30] J. Takeya, S. Akita, J. Shimoyama, and K. Kishio, Physica C **261**, 21 (1996).
[31] D. G. Cahill and R. O. Pohl, Phys. Rev. B **35**, 4067 (1987).
[32] G. Hartwig, in *Handbook of Cryogenic Engineering*, edited by J. G. Weisend II (Taylor & Francis, Philadelphia, 1998).
[33] H. B. Wang, S. Guénon, J. Yuan, A. Iishi, S. Arisawa, T. Hatano, T. Yamashita, D. Koelle, and R. Kleiner, Phys. Rev. Lett. **102**, 017006 (2009); H. B. Wang *et al.*, *ibid.* **105**, 069902 (2010).
[34] S. Guénon *et al.*, Phys. Rev. B **82**, 214506 (2010).
[35] A. Yurgens, D. Winkler, T. Claeson, S. Ono, and Y. Ando, Phys. Rev. Lett. **92**, 259702 (2004).
[36] X. B. Zhu, Y. F. Wei, S. P. Zhao, G. H. Chen, H. F. Yang, A. Z. Jin, and C. Z. Gu, Phys. Rev. B **73**, 224501 (2006).
[37] P. Hadley, M. R. Beasley, and K. Wiesenfeld, Phys. Rev. B **38**, 8712 (1988); K. Wiesenfeld, S. P. Benz, and P. A. A. Booi, J. Appl. Phys. **76**, 3835 (1994) (a review).
[38] P. Hadley, M. R. Beasley, and K. Wiesenfeld, Phys. Rev. B **38**, 8712 (1988); K. Wiesenfeld, S. P. Benz, and P. A. A. Booi, J. Appl. Phys. **76**, 3835 (1994).
[39] In fact, Josephson junctions can be synchronized even without common load, i.e., in Josephson transmission lines [see D. Tsygankov and K. Wiesenfeld, Phys. Rev. E **66**, 036215 (2002)].
[40] K. E. Gray *et al.*, IEEE Trans. Appl. Supercond. **19**, 886 (2009).